

This discussion paper is/has been under review for the journal *Climate of the Past* (CP).
Please refer to the corresponding final paper in CP if available.

Rapid changes in ice core gas records – Part 2: Understanding the rapid rise in atmospheric CO₂ at the onset of the Bølling/Allerød

P. Köhler¹, G. Knorr^{1,2}, D. Buiron³, A. Lourantou^{3,*}, and J. Chappellaz³

¹ Alfred Wegener Institute for Polar and Marine Research (AWI), P.O. Box 120161, 27515 Bremerhaven, Germany

² School of Earth and Ocean Sciences, Cardiff University, Cardiff, Wales, UK

³ Laboratoire de Glaciologie et Géophysique de l'Environnement, (LGGE, CNRS, Université Joseph Fourier-Grenoble), 54b rue Molière, Domaine Universitaire BP 96, 38402 St. Martin d'Hères, France

* now at: Laboratoire d'Océanographie et du Climat (LOCEAN), Institut Pierre Simon Laplace, Université P. et M. Curie (UPMC), Paris, France

Received: 24 June 2010 – Accepted: 26 July 2010 – Published: 11 August 2010

Correspondence to: P. Köhler (peter.koehler@awi.de)

Published by Copernicus Publications on behalf of the European Geosciences Union.

Abstract

During the last glacial/interglacial transition the Earth's climate underwent rapid changes around 14.6 kyr ago. Temperature proxies from ice cores revealed the onset of the Bølling/Allerød (B/A) warm period in the north and the start of the Antarctic Cold Reversal in the south. Furthermore, the B/A is accompanied by a rapid sea level rise of about 20 m during meltwater pulse (MWP) 1A, whose exact timing is matter of current debate. In situ measured CO₂ in the EPICA Dome C (EDC) ice core also revealed a remarkable jump of 10±1 ppmv in 230 yr at the same time. Allowing for the age distribution of CO₂ in firn we here show, that atmospheric CO₂ rose by 20–35 ppmv in less than 200 yr, which is a factor of 2–3.5 larger than the CO₂ signal recorded in situ in EDC. Based on the estimated airborne fraction of 0.17 of CO₂ we infer that 125 Pg of carbon need to be released to the atmosphere to produce such a peak. Most of the carbon might have been activated as consequence of continental shelf flooding during MWP-1A. This impact of rapid sea level rise on atmospheric CO₂ distinguishes the B/A from other Dansgaard/Oeschger events of the last 60 kyr, potentially defining the point of no return during the last deglaciation.

1 Introduction

Measurements of CO₂ over Termination I (20–10 kyr BP) from the EPICA Dome C (EDC) ice core (Monnin et al., 2001; Lourantou et al., 2010) (Fig. 1b) are temporally higher resolved and more precise than CO₂ records from other ice cores (Smith et al., 1999; Ahn et al., 2004). They have an uncertainty (1σ) of 1 ppmv (Lourantou et al., 2010) or less (Monnin et al., 2001). In these in situ measured data in EDC CO₂ rapidly rose by 10±1 ppmv between 14.74 and 14.51 kyr BP on the most recent ice core age scale (Lemieux-Dudon et al., 2010). This rapid CO₂ rise is therefore synchronous with the onset of the Bølling/Allerød (B/A) warm period in north (Steffensen et al., 2008) and the start of the Antarctic Cold Reversal in the south (Stenni et al., 2001). Furthermore,

CPD

6, 1473–1501, 2010

Rapid rise in CO₂ at the onset of the Bølling/Allerød

P. Köhler et al.

Title Page

Abstract

Introduction

Conclusions

References

Tables

Figures

⏪

⏩

◀

▶

Back

Close

Full Screen / Esc

Printer-friendly Version

Interactive Discussion



the B/A is accompanied by a rapid sea level rise of about 20 m during meltwater pulse (MWP) 1A (Peltier and Fairbanks, 2007), whose exact timing is matter of current debate (Hanebuth et al., 2000; Kienast et al., 2003; Stanford et al., 2006; Deschamps et al., 2009).

5 However, atmospheric gases trapped in ice cores are not precisely recording one point in time, but average over decades to centuries mainly depending on accumulation rate, because of the movement of gases in the firn above the close-off depth and before its enclosure in gas bubbles in the ice. An atmospheric CO₂ signal therefore has to be convoluted with the ice core specific age distribution probability density function (PDF) to gain the shape of the CO₂ signal how it might be recorded in the ice core. This age distribution PDF measuring the elapsed time since the last exchange of the CO₂ molecules with the atmosphere (Fig. 2) reveals for EDC a width between approximately 200 and 600 yr for climate conditions of pre-industrial times (PRE) and the Last Glacial Maximum (LGM), respectively (Joos and Spahni, 2008). This implicates that the CO₂ measured in situ in particular in ice cores with low accumulation rates (such as EDC) differs from the direct atmospheric signal when CO₂ changes rapidly.

In the following we will deconvolve the atmospheric CO₂ signal connected with this rapid rise in CO₂ measured in situ in the EDC ice core allowing for the age distribution PDF during the onset of the B/A. We furthermore use simulations of a global carbon cycle box model to propose which processes might have been responsible for the necessary rapid rise in atmospheric CO₂. For this final interpretation a similar effect of the age distribution PDF on CH₄ need to be considered, from which a correction of the age model is derived, to set the rapid CO₂ rise into the correct temporal context with other rapid climate changes. Details on this age correction connected with the CH₄ record are completely described in a companion paper, which is part 1 of this series of papers on rapid changes in ice core gas records (Köhler, 2010).

Rapid rise in CO₂ at the onset of the Bølling/Allerød

P. Köhler et al.

Title Page

Abstract

Introduction

Conclusions

References

Tables

Figures

◀

▶

◀

▶

Back

Close

Full Screen / Esc

Printer-friendly Version

Interactive Discussion



2 Methods

2.1 Age distribution PDF of CO₂

The age distributions PDF of CO₂ or CH₄ are functions of the climate state and the local site conditions of the ice core. Shown in Fig. 2 are distributions PDF for CO₂ for the EDC ice core for pre-industrial (PRE) and LGM conditions based on calculation with a firn densification model (Joos and Spahni, 2008). The resulting age distribution PDF for CO₂ can be approximated with reasonable accuracy ($r^2=90-94\%$) by a log-normal function (Köhler et al., 2010b):

$$y = \frac{1}{x \cdot \sigma \cdot \sqrt{2\pi}} \cdot e^{-0.5 \left(\frac{\ln(x) - \mu}{\sigma} \right)^2} \quad (1)$$

with x (yr) as the time elapsed since the last exchange with the atmosphere. This equation has two free parameters μ and σ . We chose for simplicity $\sigma=1$, which leads to an *expected value (mean)* E of the PDF of

$$E = e^{\mu - 0.5}. \quad (2)$$

The *expected value* E is in the terminology of gas physics described as *width* of the PDF, a terminology which we will also use in the following. E is different, and should not be confused with the *most likely value* defined by the location of the maximum of the PDF.

In the case of the CO₂ jump at 14.6 kyr BP one has to consider, that the atmospheric records are much younger than the surrounding ice matrix; indeed, the CO₂ jump is embedded between 473 and 480 m in glacial ice (Monnin et al., 2001; Lourantou et al., 2010) with low temperatures and low accumulation rates. However, from models of firn densification which include heat diffusion it is known that the close-off of the gas bubbles in the ice matrix is not a simple function of the temperature of the surrounding ice (Goujon et al., 2003). Heat from the surface diffuses down to the close-off region in a few centuries, depending on site-specific conditions. This implies, that atmospheric

Rapid rise in CO₂ at the onset of the Bølling/Allerød

P. Köhler et al.

Title Page

Abstract

Introduction

Conclusions

References

Tables

Figures



Back

Close

Full Screen / Esc

Printer-friendly Version

Interactive Discussion



gases during the onset of the B/A were not trapped by conditions of either the LGM or the Antarctic Cold Reversal, but by some intermediate state. New calculations with this firn densification model (Goujon et al., 2003) give a width of the PDF $E_{B/A}$ of about 400 yr with a relative uncertainty (1σ) of 14% at the onset of the B/A (Fig. 3). The width E itself varies during the jump into the B/A between 380 and 420 yr, we therefore conservatively estimate $E_{B/A}$ to lie between 320 to 480 yr with our best-guess estimate of $E_{B/A}=400$ yr.

2.2 Carbon cycle modelling

In order to determine how fast carbon injected into the atmosphere is taken up by the ocean we used the carbon cycle box model BICYCLE (Köhler and Fischer, 2004; Köhler et al., 2005a, 2010b). The model version used here and its forcing over Termination I are described in detail in Lourantou et al. (2010). We furthermore try to determine of which origin (terrestrial or marine) the carbon might have been by comparing the simulated and measured atmospheric $\delta^{13}\text{CO}_2$ fingerprint during the carbon release event. Similar approaches (identifying processes based on their $\delta^{13}\text{C}$ signature) were applied earlier for the discussion of the atmospheric $\delta^{13}\text{CO}_2$ record over the whole Termination (Lourantou et al., 2010) or longer timescales (Köhler et al., 2010b). However, the interpretation is due to the synchronous changes in both the marine and terrestrial carbon cycle during longer times more difficult than for individual rapid climate shifts, such as the onset of the B/A. In our setting here, the discussion of the general climate dynamics during Dansgaard/Oeschger (D/O) events connected with the bipolar seesaw led to reduce the B/A to the question “What process in addition to all those processes typically found during D/O events can generate such a rapid rise in CO_2 ?”

Briefly, BICYCLE consists of modules of the ocean (10 boxes distinguishing surface, intermediate and deep ocean in the Atlantic, Southern Ocean and Indo-Pacific), a globally averaged terrestrial biosphere (7 boxes), a homogenous mixed 1 box atmosphere, and a relaxation approach to account for carbonate compensation in the deep ocean

Rapid rise in CO_2 at the onset of the Bølling/Allerød

P. Köhler et al.

Title Page

Abstract

Introduction

Conclusions

References

Tables

Figures



Back

Close

Full Screen / Esc

Printer-friendly Version

Interactive Discussion



(sediment–ocean interaction). The model calculates the temporal development of its prognostic variables over time as function of changing boundary conditions, representing the climate forcing. These prognostic variables are in all boxes carbon (as dissolved inorganic carbon DIC in the ocean), $\delta^{13}\text{C}$, $\Delta^{14}\text{C}$ and additionally in the ocean boxes total alkalinity, oxygen and phosphate. The terrestrial module accounts for different photosynthetic pathways (C_3 or C_4), which is relevant for the temporal development of the ^{13}C cycle.

Here, the model is equilibrated for 4000 yr for climate conditions typical before the onset of the B/A. The Atlantic meridional overturning circulation (AMOC) is in an off mode. Besides the carbon injection described below, the terrestrial carbon content is assumed to stay constant. The simulated jump of CO_2 is then generated by the injection of carbon into the atmosphere in 50, 100, 150, 200, 250 or 300 yr being either of terrestrial or marine origin. The two scenarios of C injection into the atmosphere differ only in their carbon isotopic signature:

Terrestrial scenario: The $\delta^{13}\text{C}$ signature is based on a study with a global dynamical vegetation model (Scholze et al., 2003), which calculates for present day a mean global isotopic fractionation of the terrestrial biosphere of 17.7‰. We have to consider a larger fraction of C_4 plants during colder climates and lower atmospheric $p\text{CO}_2$ (Coltatz et al., 1998) as found at the onset of the B/A. This implies that about 20 and 30% of the terrestrial carbon is of C_4 origin for present day and LGM, respectively (Köhler and Fischer, 2004). The significantly smaller isotopic fractionation during C_4 photosynthesis (about 5‰) in comparison to C_4 photosynthesis (about 20‰) (Lloyd and Farquhar, 1994) therefore reduces this global mean terrestrial fractionation to 16‰. With an atmospheric $\delta^{13}\text{CO}_2$ signature of about -6.5‰ the terrestrial biosphere has a mean $\delta^{13}\text{C}$ signature of -22.5‰ .

Marine scenario: In this scenario we assume that old carbon from the deep ocean heavily depleted in $\delta^{13}\text{C}$ might upwell and outgas to the atmosphere. Today's values of oceanic $\delta^{13}\text{C}$ in the deep Pacific are about 0.0‰ (Kroopnick, 1985). From reconstructions (Boyle, 1992) it is known, that during the LGM deep ocean $\delta^{13}\text{C}$ was on average

Rapid rise in CO_2 at the onset of the Bølling/Allerød

P. Köhler et al.

[Title Page](#)[Abstract](#)[Introduction](#)[Conclusions](#)[References](#)[Tables](#)[Figures](#)[⏪](#)[⏩](#)[◀](#)[▶](#)[Back](#)[Close](#)[Full Screen / Esc](#)[Printer-friendly Version](#)[Interactive Discussion](#)

not more than about 0.5‰ smaller, thus $\delta^{13}\text{C}_{\text{LGM}} = -0.5\text{‰}$. During out-gassing a net isotopic fractionation of 8‰ has to be considered (Siegenthaler and Münnich, 1981), leading to $\delta^{13}\text{C} = -8.5\text{‰}$ in the carbon injected into the atmosphere if of marine origin.

The signal of simulated atmospheric CO_2 and $\delta^{13}\text{CO}_2$ plotted in the figures are derived by subtracting simulated CO_2 and $\delta^{13}\text{CO}_2$ of a reference run without carbon injections from our scenarios. The anomalies $\Delta(\text{CO}_2)$ and $\Delta(\delta^{13}\text{CO}_2)$ are then added to the starting point of the CO_2 jump ($\delta^{13}\text{CO}_2$ drop) into the B/A, which we define as 228 ppmv (-6.757‰) at 14.8 kyr BP. In doing so, existing equilibration trends (which will exist even for longer equilibration periods due to the sediment-ocean interaction) are eliminated. Simulated atmospheric CO_2 ($\delta^{13}\text{CO}_2$) at the end of the equilibration period was 223 ppmv (-6.54‰). Our modelling exercise is therefore only valid for an interpretation of the rapid CO_2 rise of 10 ppmv in the in situ data of EDC. The mismatch in CO_2 and $\delta^{13}\text{CO}_2$ between simulations and EDC data before 15 kyr BP and after 14.2 kyr BP is therefore expected (Figs. 4b,d, 5b,d, 7).

3 Results and discussions

3.1 Fingerprint analysis and process detection

We first estimate roughly the amount of carbon necessary to be injected as CO_2 into the atmosphere to produce a long-term jump of 10 ppmv using the airborne fraction f . The long-term (centuries to millenia) airborne fraction f of CO_2 can be approximated from the buffer or Revelle factor (RF) of the ocean on atmospheric $p\text{CO}_2$ rise. The present day mean surface ocean Revelle factor (Sabine et al., 2004a) is about 10. With

$$\text{RF} = \frac{\Delta p\text{CO}_2 / p\text{CO}_2}{\Delta \text{DIC} / \text{DIC}} \quad (3)$$

Rapid rise in CO_2 at the onset of the Bølling/Allerød

P. Köhler et al.

Title Page

Abstract

Introduction

Conclusions

References

Tables

Figures

◀

▶

◀

▶

Back

Close

Full Screen / Esc

Printer-friendly Version

Interactive Discussion



and the content of C in the atmosphere at the beginning of the B/A ($C_A=500 \text{ Pg C} \approx 235 \text{ ppmv}$) and in the ocean ($C_O=37\,500 \text{ Pg C}=75 \cdot C_A$) it is

$$f = \frac{\Delta p\text{CO}_2}{\Delta p\text{CO}_2 + \Delta \text{DIC}} = \frac{1}{1 + \frac{75}{\text{RF}}} = 0.118. \quad (4)$$

Thus, the lower end of the range of the airborne fraction f is about 12% (given by Eq. 4), while the upper end of the range might be derived from modern anthropogenic fossil fuel emissions (Le Quéré et al., 2009) to about 45%. Please note, that f estimated with Eq. (4) assumes a passive (constant) terrestrial biosphere, while in the estimate of f from fossil fuel emissions (Le Quéré et al., 2009) the terrestrial carbon cycle is assumed to take up about a third of the anthropogenic C emissions. We take the range of f between 12 and 45% as a first order approximation and assume f during the B/A to lie in-between. This implies that a long-term rise in atmospheric CO_2 of 10 ppmv (equivalent to a rise in the atmospheric C reservoir by 21.2 Pg C) can be generated by the injection of 47 to 180 Pg C into the atmosphere.

We further refine this amplitude to 125 Pg C (equivalent to $f=17\%$) by using the global carbon cycle box model BICYCLE. The model then generates atmospheric CO_2 peaks of 20–35 ppmv, depending on the abruptness of the C injection (Fig. 4a). All scenarios with release times of 50–200 yr fulfil the EDC ice core data requirements after the application of the age distribution PDF (Fig. 4b). The acceptable scenarios imply rates of change in atmospheric CO_2 of 13–70 ppmv per century, a factor of 3–16 higher than in the EDC data. Our fastest scenario (release time of 50 yr) has a rate of change in atmospheric CO_2 , which is still a factor of two smaller than the anthropogenic CO_2 rise of 70 ppmv during the last 50 yr (Keeling et al., 2009). For comparison, in the less precise CO_2 data points taken from the Taylor Dome (Smith et al., 1999) and Siple Dome (Ahn et al., 2004) ice cores the B/A CO_2 jump is recorded with 15 ± 2 and 19 ± 4 ppmv, respectively (Fig. 4a), with changing rates in ice core CO_2 of $\sim 4\text{--}6$ ppmv per century.

Rapid rise in CO_2 at the onset of the Bølling/Allerød

P. Köhler et al.

Title Page

Abstract

Introduction

Conclusions

References

Tables

Figures

◀

▶

◀

▶

Back

Close

Full Screen / Esc

Printer-friendly Version

Interactive Discussion



The uncertainty in the size of the CO₂ peak given by the variability in the width $E_{B/A}$ of the age distribution PDF and by the range in the airborne fraction f lead to slightly different results. The differences in $E_{B/A}$ between 320 and 480 yr give for $f=0.17$ variations in the atmospheric CO₂ peak height of less than 1 ppmv from the standard case and these results are still within uncertainties of the ice core data (Fig. 5b). We show in Fig. 5a,c how the atmospheric CO₂ and $\delta^{13}\text{CO}_2$ would look like for the upper (45%) and lower (12%) end-of-range values in the airborne fraction f , if simulated with our carbon cycle box model. The signal potentially recorded in EDC is achieved after applying the age distribution PDF (Fig. 5b,d). Atmospheric CO₂ rises only by 10 ppmv in the 47 Pg C-scenario, which would potentially be recorded as 4 ppmv in EDC. In the 180 Pg C-scenario the CO₂ amplitude in the atmosphere would be 13 ppmv larger than in our reference case, leading to a long-term CO₂ jump of 16 ppmv in a hypothetical EDC ice core. Both extreme cases for f are after the application of the age distribution PDF not in line with the evidence from the ice core data.

But what generated this jump of CO₂ into the B/A? Changes in near-surface temperature and in AMOC have massive impacts on the reorganisation of the terrestrial and the marine carbon cycle (Köhler et al., 2005b; Schmittner and Galbraith, 2008), respectively. This leads to CO₂ amplitudes of about 20 ppmv during D/O events (Ahn and Brook, 2008). At the onset of the B/A the temperature changes in the northern and southern high latitudes as recorded in Greenland and in the central Antarctic plateau follow the typical pattern of the bipolar seesaw that also characterises the last glacial cycle (EPICA-community-members, 2006; Barker et al., 2009): gradual warming in the south during a stadial cold phase in the north switches to gradual cooling at the onset of a rapid temperature rise in the north (Fig. 1A). These interhemispheric pattern were identified for all D/O events during Marine Isotope Stage 3 (MIS 3) and for the B/A as D/O event 1 (EPICA-community-members, 2006) (Fig. 1). In contrast to all D/O events during MIS 3, in which CO₂ started to decline at the onset of Greenland warming (Ahn and Brook, 2008), CO₂ rapidly increased around 14.6 kyr BP. This strongly suggests that changes in the AMOC are not the main source of the detected CO₂ jump at the

Rapid rise in CO₂ at the onset of the Bølling/Allerød

P. Köhler et al.

Title Page

Abstract

Introduction

Conclusions

References

Tables

Figures

◀

▶

◀

▶

Back

Close

Full Screen / Esc

Printer-friendly Version

Interactive Discussion



onset of the B/A, since the general trend of the CO₂ evolution during the other D/O events in MIS 3 is of opposite sign.

To constrain the origin of the released carbon further we investigate the two hypotheses, that the carbon was only of either terrestrial or marine origin. Our two scenarios vary only in the isotopic signature of the injected C (terrestrial: $\delta^{13}\text{CO}_2 = -22.5\text{‰}$, marine: $\delta^{13}\text{CO}_2 = -8.5\text{‰}$). We compare carbon cycle model simulations of the typical fingerprint of these two hypotheses with new measurements of atmospheric $\delta^{13}\text{CO}_2$ from EDC (Lourantou et al., 2010). We find that the small dip of $-0.14 \pm 0.14\text{‰}$ in $\delta^{13}\text{CO}_2$ measured in situ in EDC might be generated by terrestrial C released in less than three centuries (Fig. 4c,d). The marine scenario leads to changes in $\delta^{13}\text{CO}_2$ of less than -0.03‰ (Fig. 4d). Within the uncertainty in so far published ice core $\delta^{13}\text{CO}_2$ of 0.10‰ (1σ) this marine scenario seems less likely than the terrestrial one, but it can not be excluded. All-together, this $\delta^{13}\text{CO}_2$ fingerprint analysis shows that all possible terrestrial or marine scenarios seemed to be possible, but a further constrain is based on the given data so far not possible.

Besides the similarity in the typical patterns of the bipolar seesaw the B/A and the other D/O events differ significantly in the rate of sea level rise. While the amplitudes of sea level variations are with about 20 m during MIS 3 and B/A comparable (Peltier and Fairbanks, 2007; Siddall et al., 2008) the rates of change are not. It took one to several millennia for the sea level to change during MIS 3 (rate of change of 1–2 m per century, Siddall et al., 2008), but during MWP-1A sea level rose by more than 5 m per century accumulating 16 to 20 m of sea level rise within centuries (Peltier and Fairbanks, 2007; Hanebuth et al., 2000). The exact magnitude but also the timing of the sea level rise during MWP-1A varies depending on site location and reconstruction method. However, Sunda Shelf data (Hanebuth et al., 2000; Kienast et al., 2003) and recent evidence from Tahiti (Deschamps et al., 2009) point to a timing of MWP-1A at 14.6 kyr BP, in parallel to the temperature rise and the jump in CO₂ into the B/A. Sea level records (Thompson and Goldstein, 2007) suggest that large shelf areas which were submerged the last time around 30 kyr BP were flooded by MWP-1A 15 kyr later

Rapid rise in CO₂ at the onset of the Bølling/Allerød

P. Köhler et al.

[Title Page](#)[Abstract](#)[Introduction](#)[Conclusions](#)[References](#)[Tables](#)[Figures](#)[Back](#)[Close](#)[Full Screen / Esc](#)[Printer-friendly Version](#)[Interactive Discussion](#)

within centuries. The terrestrial ecosystems had thus ample time to develop dense vegetation and accumulate huge amounts of carbon, which could thus be released rapidly. In contrast to MWP-1A the gradual sea level rise during MIS 3 allowed for CO₂ equilibration between atmosphere and ocean.

5 We estimate from bathymetry (Smith and Sandwell, 1997) that 2.2, 3.2 or 4.0×10¹² m² of land were flooded during MWP-1A for sea level rising between –96 m and –70 m by 16, 20 or 26 m, respectively. This covers the different reconstructions published for MWP-1A (from –96 m to –80 m, from –90 m to –70 m, or a combination of both, Hanebuth et al., 2000; Peltier and Fairbanks, 2007). It ignores differences in sea
10 level rise due to the local effects such as continental uplift or subduction and the relative position with respect to the entry point of waters responsible for MWP-1A. About 23% of the flooded areas (Fig. 6) are located in the tropics (20° S to 20° N). To calculate the upper limit of the amount of carbon potentially released by shelf flooding during MWP-1A we assume present day carbon storage densities typically for tropical rain
15 forests (60 kg m⁻²) for the tropical belt and the global mean (20 kg m⁻²) for all other areas (Sabine et al., 2004b). Depending on the assumed sea level rise mentioned above we estimate that up to 64, 94 or 116 Pg C (equivalent to 51 to 93% of the necessary C injection) might have been stored on those lands flooded during MWP-1A with about 50% located in the tropical belt. This estimate includes a complete relocation
20 of the carbon stored on the flooded shelves to the atmosphere without any significant time delay. The efficiency of this “flooding-scenario” is dependent on the relative timing of MWP-1A. Several studies have indicated a time window between the onset of the B/A and the Older Dryas, i.e. between about 14.7 and 14 kyr BP (Stanford et al., 2006; Hanebuth et al., 2000; Kienast et al., 2003; Peltier and Fairbanks, 2007), including scenarios that place MWP-1A right at the onset of the B/A (Hanebuth et al., 2000; Kienast
25 et al., 2003; Deschamps et al., 2009).

To set the timing of the rapid rise in atmospheric CO₂ into the temporal context with MWP-1A one has to consider, that the recent ice core age model used here (Lemieux-Dudon et al., 2010) is based on the synchronisation of CH₄ measured in situ

CPD

6, 1473–1501, 2010

Rapid rise in CO₂ at the onset of the Bølling/Allerød

P. Köhler et al.

Title Page

Abstract

Introduction

Conclusions

References

Tables

Figures

◀

▶

◀

▶

Back

Close

Full Screen / Esc

Printer-friendly Version

Interactive Discussion



in various ice cores. Accounting for a similar age distribution PDF in CH₄ than in CO₂ the rapid CH₄ rise at the onset of the B/A is recorded in EDC about 200 yr later than in the Greenland ice core NGRIP, which depicts due to its high accumulation rate the atmospheric CH₄ signal with only a very small temporal offset (Köhler, 2010). If corrected for this CH₄ synchronisation artefact the proposed atmospheric rise in CO₂ then starts around 14.6 kyr BP, in perfect agreement with the possible dating of MWP-1A (Fig. 7).

The residual carbon needs to be related to other processes. From the discussed comparison of the B/A with other D/O events during MIS 3 it emerged that processes directly related to the bipolar temperature seesaw (e.g. enhanced northern hemispheric soil respiration due to warming or vegetation displacements (Köhler et al., 2005b), marine productivity changes (Schmittner and Galbraith, 2008) connected with changes in the AMOC) are unlikely candidates, because they should also have been in operation during those other D/O events and would then have led to a similar carbon release. The origin of the water masses responsible for MWP-1A is still discussed (Peltier, 2005). If a main fraction of the waters was of northern origin and released during a retreat (not a thinning) of northern hemispheric ice sheets then the release of carbon potentially buried underneath ice sheets following the glacial burial hypothesis (Zeng, 2007) might be considered. This might, however, be counteracted by enhanced carbon sequestration on new land areas available at the southern edge of the retreating ice sheets. Both processes are irrelevant for retreating ice sheets in Antarctica. The generation of new wet lands at the onset of the B/A, as corroborated by the isotopic signature of $\delta^{13}\text{CH}_4$ points to a unique redistribution of the land carbon cycle during that time (Fischer et al., 2008). Furthermore, a potential contribution from the ocean might also be necessary. However, a quantification of these processes is not in the scope of this study.

The rate of change in CO₂ at the onset of the B/A is not unique for the last glacial cycle. In the time window 65–90 kyr BP (belonging to MIS 4 and 5) CO₂ measured in situ in the Byrd ice core (Ahn and Brook, 2008) rose several times rapidly by up to 22±4 ppmv in 200 yr, sometimes synchronous with northern warming (similar as for

Rapid rise in CO₂ at the onset of the Bølling/Allerød

P. Köhler et al.

Title Page

Abstract

Introduction

Conclusions

References

Tables

Figures

◀

▶

◀

▶

Back

Close

Full Screen / Esc

Printer-friendly Version

Interactive Discussion



the B/A), and sometimes not. It needs to be tested if a similar flooding mechanism as proposed here was also responsible for these CO₂ jumps.

3.2 Some more thoughts on carbon released from shelf flooding

To our knowledge there exists so far no study, how carbon stored on land would be released in detail by flooding events. Our first order approximation given here is therefore based on the assumption that all carbon stored on land is released immediately to the atmosphere. In the following we like to support this view with simple thought experiments and highlight potential delays.

Our understanding of shelf flooding is as follows: A rising sea level with a rate of rise of more than 5 m per century typical for MWP-1A would be superimposed on higher frequency sea level variabilities such as tides. This would during short sea level high stands (e.g., spring tides) successively threatens salt-intolerant plant species established on the flooded land area. The individual plants of these salt-intolerant species would be the first to die after sufficient exposure to salt-water conditions even after the water retreat following the spring tide. Finally all previously established land species, which are supposed to rely on freshwater conditions, will die and decay. The decay of foliage is rapid (less than a 1 yr), while that of hard wood might take considerably longer (about 25 yr in a terrestrial biosphere module, Köhler and Fischer, 2004). Heterotrophic respired carbon fluxes of dead vegetation goes dominantly to the detritus and partially to the atmosphere and soil pools. Detritus itself has a turn over times of a few years only. Most soil carbon pools have a turnover time of less than one century. We therefore imagine that after the collapse of the vegetation, which implies a stop in the carbon input into the soil, most soil carbon is released to the atmosphere in less than a century. Our estimate that 50% of the released carbon was originated in the tropics would allow for an even faster injection of carbon into the atmosphere, because respiration rates are temperature dependent and much faster (turnover times much smaller) in the warm and humid tropics than in boreal regions. How the final soil carbon release is affected by rising sea level and thus salt water conditions depends on the temporal

Rapid rise in CO₂ at the onset of the Bølling/Allerød

P. Köhler et al.

Title Page

Abstract

Introduction

Conclusions

References

Tables

Figures



Back

Close

Full Screen / Esc

Printer-friendly Version

Interactive Discussion



offset between the vegetation collapse and the start of a long-term influence of salty waters on the soil. Following the spring tide idea above, this temporal offset might be substantially, e.g. some decades. All-together, the carbon released from flooded shelves might include nearly the complete standing stocks and should not be delayed by more than a century.

4 Conclusions

Our analysis provides evidence that the atmospheric CO₂ at the onset of the B/A includes a rise of 20–35 ppmv within less than two centuries. This needs further investigations in sophisticated carbon cycle-climate models, because its radiative feedback alone causes a global temperature rise of up to 0.25 K, which other feedbacks might amplify substantially (Köhler et al., 2010a). Based on the dynamical linkage between the temperature rise at the onset of the B/A, the changes in the AMOC and MWP-1A we have provided an explanation for the CO₂ jump, which is distinct from the CO₂ signature during other D/O events in MIS 3, potentially defining the point of no return during the last deglaciation. The mechanism of continental shelf flooding might also be relevant for future climate change given the range of sea level projections in response to rising global temperature and potential instabilities of the Greenland and the West Antarctic ice sheets (Lenton et al., 2008). In analogy to the identified deglacial sequence such an instability might amplify the anthropogenic CO₂ rise.

Acknowledgements. We thank Hubertus Fischer for discussions and for pointing us at the question of strong terrestrial carbon changes during rapid CO₂ jumps. Johannes Freitag provided us with insights to gases in firn and related difficulties in dating ice core gas records. Renato Spahni provided the gas age distribution calculated with a firn densification model plotted in Fig. 2 and in-depth details on gas chronologies.

Rapid rise in CO₂ at the onset of the Bølling/Allerød

P. Köhler et al.

Title Page

Abstract

Introduction

Conclusions

References

Tables

Figures

◀

▶

◀

▶

Back

Close

Full Screen / Esc

Printer-friendly Version

Interactive Discussion



References

- Ahn, J. and Brook, E. J.: Atmospheric CO₂ and climate on millennial time scales during the last glacial period, *Science*, 322, 83–85, doi:10.1126/science.1160832, 2008. 1481, 1484, 1493
- Ahn, J., Wahlen, M., Deck, B. L., Brook, E. J., Mayewski, P. A., Taylor, K. C., and White, J. W. C.:
5 A record of atmospheric CO₂ during the last 40 000 years from the Siple Dome, Antarctica ice core, *J. Geophys. Res.*, 109, D13305, doi:10.1029/2003JD004415, 2004. 1474, 1480, 1497
- Barker, S., Diz, P., Vantravers, M. J., Pike, J., Knorr, G., Hall, I. R., and Broecker, W. S.: Inter-hemispheric Atlantic seesaw response during the last deglaciation, *Nature*, 457, 1007–1102, doi:10.1038/nature07770, 2009. 1481
- 10 Boyle, E. A.: Cadmium and $\delta^{13}\text{C}$ paleochemical ocean distributions during the stage 2 glacial maximum, *Ann. Rev. Earth Planet. Sci.*, 20, 245–287, 1992. 1478
- Collatz, G. J., Berry, J. A., and Clark, J. S.: Effects of climate and atmospheric CO₂ partial pressure on the global distribution of C₄ grasses: present, past and future, *Oecologia*, 114, 441–454, 1998. 1478
- 15 Deschamps, P., Durand, N., Bard, E., Hamelin, B., Camoin, G., Thomas, A., Henderson, G., and Yokoyama, Y.: Synchronicity of Meltwater Pulse 1A and the Bolling onset: New evidence from the IODP Tahiti Sea-Level Expedition, *Geophys. Res. Abstr.*, 11, EGU22009–10233, 2009. 1475, 1482, 1483
- 20 EPICA-community-members: One-to-one coupling of glacial climate variability in Greenland and Antarctica, *Nature*, 444, 195–198, doi:10.1038/nature05301, 2006. 1481
- Fischer, H., Behrens, M., Bock, M., Richter, U., Schmitt, J., Loulergue, L., Chappellaz, J., Spahni, R., Blunier, T., Leuenberger, M., and Stocker, T. F.: Changing boreal methane sources and constant biomass burning during the last termination, *Nature*, 452, 864–867, doi:10.1038/nature06825, 2008. 1484
- 25 Goujon, C., Barnola, J.-M., and Ritz, C.: Modeling the densification of polar firn including heat diffusion: Application to close-off characteristics and gas isotopic fractionation for Antarctica and Greenland sites, *J. Geophys. Res.*, 108, 4792, doi:10.1029/2002JD003319, 2003. 1476, 1477, 1495, 1499
- 30 Hanebuth, T., Statterger, K., and Grootes, P. M.: Rapid flooding of the Sunda Shelf: a late-glacial sea-level record, *Science*, 288, 1033–1035, doi:10.1126/science.288.5468.1033, 2000. 1475, 1482, 1483, 1493, 1501

Rapid rise in CO₂ at the onset of the Bolling/Allerød

P. Köhler et al.

Title Page

Abstract

Introduction

Conclusions

References

Tables

Figures

◀

▶

◀

▶

Back

Close

Full Screen / Esc

Printer-friendly Version

Interactive Discussion



Rapid rise in CO₂ at the onset of the Bølling/Allerød

P. Köhler et al.

Title Page

Abstract

Introduction

Conclusions

References

Tables

Figures

◀

▶

◀

▶

Back

Close

Full Screen / Esc

Printer-friendly Version

Interactive Discussion



- Joos, F. and Spahni, R.: Rates of change in natural and anthropogenic radiative forcing over the past 20 000 years, *Proc. Natl. Acad. Sci.*, 105, 1425–1430, doi:10.1073/pnas.0707386105, 2008. 1475, 1476, 1494, 1495
- Keeling, R. F., Piper, S., Bollenbacher, A., and Walker, J.: Atmospheric CO₂ records from sites in the SIO air sampling network, in: *Trends: A Compendium of Data on Global Change, Carbon Dioxide Information Analysis Center, Oak Ridge National Laboratory, US Department of Energy, Oak Ridge, Tenn., USA, 2009.* 1480
- Kienast, M., Hanebuth, T., Pelejero, C., and Steinke, S.: Synchronicity of meltwater pulse 1a and the Bølling warming: New evidence from the South China Sea, *Geology*, 31, 67–70, 2003. 1475, 1482, 1483, 1501
- Köhler, P.: Rapid changes in ice core gas records – Part 1: On the accuracy of methane synchronisation of ice cores, *Clim. Past Discuss.*, 6, 1453–1471, doi:10.5194/cpd-6-1453-2010, 2010. 1475, 1484, 1501
- Köhler, P. and Fischer, H.: Simulating changes in the terrestrial biosphere during the last glacial/interglacial transition, *Global Planet. Change*, 43, 33–55, doi:10.1016/j.gloplacha.2004.02.005, 2004. 1477, 1478, 1485
- Köhler, P., Fischer, H., Munhoven, G., and Zeebe, R. E.: Quantitative interpretation of atmospheric carbon records over the last glacial termination, *Global Biogeochem. Cy.*, 19, GB4020, doi:10.1029/2004GB002345, 2005a. 1477
- Köhler, P., Joos, F., Gerber, S., and Knutti, R.: Simulated changes in vegetation distribution, land carbon storage, and atmospheric CO₂ in response to a collapse of the North Atlantic thermohaline circulation, *Clim. Dynam.*, 25, 689–708, doi:10.1007/s00382-005-0058-8, 2005b. 1481, 1484
- Köhler, P., Bintanja, R., Fischer, H., Joos, F., Knutti, R., Lohmann, G., and Masson-Delmotte, V.: What caused Earth's temperature variations during the last 800 000 years? Data-based evidences on radiative forcing and constraints on climate sensitivity, *Quaternary Sci. Rev.*, 29, 129–145, doi:10.1016/j.quascirev.2009.09.026, 2010a. 1486
- Köhler, P., Fischer, H., and Schmitt, J.: Atmospheric $\delta^{13}\text{CO}_2$ and its relation to $p\text{CO}_2$ and deep ocean $\delta^{13}\text{C}$ during the late Pleistocene, *Paleoceanography*, 25, PA1213, doi:10.1029/2008PA001703, 2010b. 1476, 1477
- Kroopnick, P. M.: The distribution of ^{13}C of $\sum\text{CO}_2$ in the world oceans, *Deep-Sea Res. Pt. I*, 32, 57–84, 1985. 1478
- Le Quééré, C., Raupach, M. R., Canadell, J. G., Marland, G., Bopp, L., Ciais, P., Conway, T. J.,

Rapid rise in CO₂ at the onset of the Bølling/Allerød

P. Köhler et al.

[Title Page](#)[Abstract](#)[Introduction](#)[Conclusions](#)[References](#)[Tables](#)[Figures](#)[Back](#)[Close](#)[Full Screen / Esc](#)[Printer-friendly Version](#)[Interactive Discussion](#)

Doney, S. C., Feely, R. A., Foster, P., Friedlingstein, P., Gurney, K., Houghton, R. A., House, J. I., Huntingford, C., Levy, P. E., Lomas, M. R., Majku, J., Metz, N., Ometto, J. P., Peters, G. P., Prentice, I. C., Randerson, J. T., Running, S. W., Sarmiento, J. L., Schuster, U., Sitch, S., Takahashi, T., Viovy, N., van der Werf, G. R., and Woodward, F. I.: Trends in the sources and sinks of carbon dioxide, *Nat. Geosci.*, 2, 831–836, doi:10.1038/ngeo689, 2009. 1480

Lemieux-Dudon, B., Blayo, E., Petit, J.-R., Waelbroeck, C., Svensson, A., Ritz, C., Barnola, J.-M., Narcisi, B. M., and Parrenin, F.: Consistent dating for Antarctic and Greenland ice cores, *Quaternary Sci. Rev.*, 29, 8–20, doi:10.1016/j.quascirev.2009.11.010, 2010. 1474, 1483, 1493, 1495, 1497, 1501

Lenton, T. M., Held, H., Kriegler, E., Hall, J. W., Lucht, W., Rahmstorf, S., and Schellnhuber, H. J.: Tipping elements in the Earth's climate system, *Proc. Natl. Acad. Sci.*, 105, 1786–1793, doi:10.1073/pnas.0705414, 105, 2008. 1486

Lloyd, J. and Farquhar, G. D.: ¹³C discrimination during CO₂ assimilation by the terrestrial biosphere, *Oecologia*, 99, 201–215, 1994. 1478

Lourantou, A., Lavrič, J. V., Köhler, P., Barnola, J.-M., Michel, E., Paillard, D., Raynaud, D., and Chappellaz, J.: Constraint of the CO₂ rise by new atmospheric carbon isotopic measurements during the last deglaciation, *Global Biogeochem. Cy.*, 24, GB2015, doi:10.1029/2009GB003545, 2010. 1474, 1476, 1477, 1482, 1493, 1495, 1497

Monnin, E., Indermühle, A., Dällenbach, A., Flückiger, J., Stauffer, B., Stocker, T. F., Raynaud, D., and Barnola, J.-M.: Atmospheric CO₂ concentrations over the last glacial termination, *Science*, 291, 112–114, 2001. 1474, 1476, 1493, 1495, 1497

NorthGRIP-members: High-resolution record of Northern Hemisphere climate extending into the last interglacial period, *Nature*, 431, 147–151, 2004. 1493

Peltier, W. R.: On the hemispheric origin of meltwater pulse 1a, *Quaternary Sci. Rev.*, 24, 1655–1671, 2005. 1484

Peltier, W. R. and Fairbanks, R. G.: Global glacial ice volume and Last Glacial Maximum duration from an extended Barbados sea level record, *Quaternary Sci. Rev.*, 25, 3322–3337, doi:10.1016/j.quascirev.2006.04.010, 2007. 1475, 1482, 1483, 1493

Sabine, C. L., Feely, R. A., Gruber, N., Key, R. M., Lee, K., Bullister, J. L., Wanninkhof, R., Wong, C. S., Wallace, D. W. R., Tilbrook, B., Millero, F. J., Peng, T.-H., Kozyr, A., Ono, T., and Rios, A. F.: The oceanic sink for anthropogenic CO₂, *Science*, 305, 367–371, 2004a. 1479

Sabine, C. L., Heimann, M., Artaxo, P., Bakker, D. C. E., Arthur, C.-T., Field, C. B., Gruber, N., Le

Rapid rise in CO₂ at the onset of the Bølling/Allerød

P. Köhler et al.

Title Page

Abstract

Introduction

Conclusions

References

Tables

Figures



Back

Close

Full Screen / Esc

Printer-friendly Version

Interactive Discussion



Quééré, C., Prinn, R. G., Richey, J. E., Lankao, P. R., Sathaye, J. A., and Valentini, R.: Current status and past trends of the global carbon cycle, in: *The Global Carbon Cycle: Integrating Humans, Climate, and the Natural World*, edited by: Field, C. B. and Raupach, M. R., Island Press, Washington, Covelo, London, 17–44, 2004b. 1483

5 Schmittner, A. and Galbraith, E. D.: Glacial greenhouse-gas fluctuations controlled by ocean circulation changes, *Nature*, 456, 373–376, doi:10.1038/nature07531, 2008. 1481, 1484

Scholze, M., Kaplan, J. O., Knorr, W., and Heimann, M.: Climate and interannual variability of the atmosphere-biosphere ¹³CO₂ flux, *Geophys. Res. Lett.*, 30, 1097, doi:10.1029/2002GL015631, 2003. 1478

10 Siddall, M., Rohling, E. J., Thompson, W. G., and Waelbroeck, C.: Marine isotope stage 3 sea level fluctuations: data synthesis and new outlook, *Rev. Geophys.*, 46, RG4003, doi:10.1029/2007RG000226, 2008. 1482, 1493

Siegenthaler, U. and Münnich, K. O.: ¹³C/¹²C fractionation during CO₂ transfer from air to sea, in: *Carbon Cycle Modelling*, edited by: Bolin, B., vol. 16 of SCOPE, Wiley and Sons, Chichester, NY, 249–257, 1981. 1479

15 Smith, H. J., Fischer, H., Wahlen, M., Mastroianni, D., and Deck, B.: Dual modes of the carbon cycle since the Last Glacial Maximum, *Nature*, 400, 248–250, 1999. 1474, 1480, 1497

Smith, W. H. and Sandwell, D. T.: Global sea floor topography from satellite altimetry and ship depth soundings, *Science*, 277, 1956–1962, doi:10.1126/science.277.5334.1956, 1997. 1483, 1500

20 Spahni, R., Chappellaz, J., Stocker, T. F., Loulergue, L., Hausammann, G., Kawamura, K., Flückiger, J., Schwander, J., Raynaud, D., Masson-Delmotte, V., and Jouzel, J.: Atmospheric methane and nitrous oxide of the late Pleistocene from Antarctic ice cores, *Science*, 310, 1317–1321, doi:10.1126/science.1120132, 2005. 1493

25 Stanford, J. D., Rohling, E. J., Hunter, S. E., Roberts, A. P., Rasmussen, S. O., Bard, E., McManus, J., and Fairbanks, R. G.: Timing of meltwater pulse 1a and climate responses to meltwater injections, *Paleoceanography*, 21, PA4103, doi:10.1029/2006PA001340, 2006. 1475, 1483

30 Steffensen, J. P., Andersen, K. K., Bigler, M., Clausen, H. B., Dahl-Jensen, D., Fischer, H., Goto-Azuma, K., Hansson, M., Johnsen, S. J., Jouzel, J., Masson-Delmotte, V., Popp, T., Rasmussen, S. O., Rothlisberger, R., Ruth, U., Stauffer, B., Siggaard-Andersen, M.-L., Sveinbjörnsdóttir, A. E., Svensson, A., and White, J. W. C.: High-resolution Greenland ice core data show abrupt climate change happens in few years, *Science*, 321, 680–684,

doi:10.1126/science.1157707, 2008. 1474

Stenni, B., Masson-Delmotte, V., Johnsen, S., Jouzel, J., Longinelli, A., Monnin, E., Röthlisberger, R., and Selmo, E.: An oceanic cold reversal during the last deglaciation, *Science*, 293, 2074–2077, 2001. 1474, 1493, 1495

5 Thompson, W. G. and Goldstein, S. L.: A radiometric calibration of the SPECMAP timescale, *Quaternary Sci. Rev.*, 25, 3207–3206, doi:10.1016/j.quascirev.2006.02.007, 2007. 1482, 1493

Zeng, N.: Quasi-100 ky glacial-interglacial cycles triggered by subglacial burial carbon release, *Clim. Past*, 3, 135–153, doi:10.5194/cp-3-135-2007, 2007. 1484

Rapid rise in CO₂ at the onset of the Bølling/Allerød

P. Köhler et al.

Title Page

Abstract

Introduction

Conclusions

References

Tables

Figures



Back

Close

Full Screen / Esc

Printer-friendly Version

Interactive Discussion



Rapid rise in CO₂ at the onset of the Bølling/Allerød

P. Köhler et al.

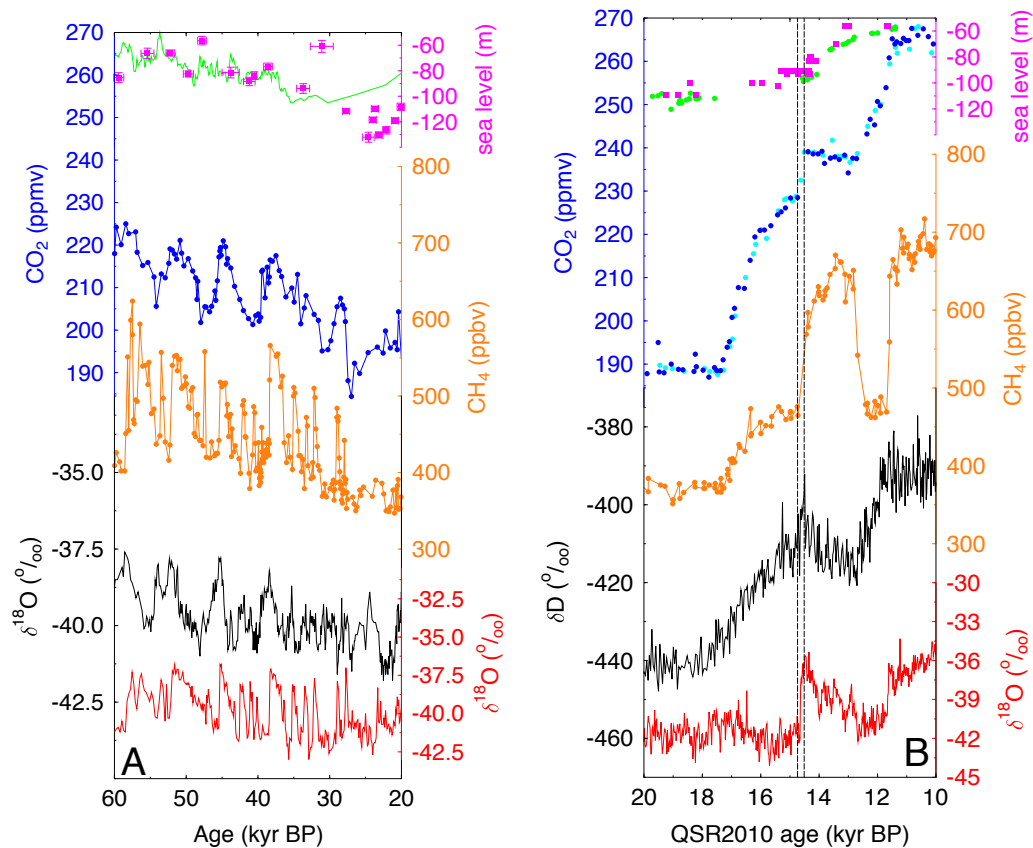


Fig. 1.

Title Page

Abstract

Introduction

Conclusions

References

Tables

Figures

◀

▶

◀

▶

Back

Close

Full Screen / Esc

Printer-friendly Version

Interactive Discussion



Rapid rise in CO₂ at the onset of the Bølling/Allerød

P. Köhler et al.

Title Page

Abstract

Introduction

Conclusions

References

Tables

Figures

◀

▶

◀

▶

Back

Close

Full Screen / Esc

Printer-friendly Version

Interactive Discussion



Fig. 1. Climate records during MIS 3 and Termination I. From top to bottom: relative sea level, CO₂, CH₄ and isotopic temperature proxies (δD or $\delta^{18}O$) from Antarctica (black) and Greenland (red). **(A)** MIS 3 data from the Byrd and GISP2 ice cores (Ahn and Brook, 2008) and sea level from a compilation (magenta) based on coral reef terraces (Thompson and Goldstein, 2007) and the synthesis (green) from the Red Sea method (Siddall et al., 2008). **(B)** Termination I data from the EDC and NGRIP ice cores (Monnin et al., 2001; Spahni et al., 2005; Stenni et al., 2001; NorthGRIP-members, 2004; Lourantou et al., 2010) Previous (Monnin et al., 2001) (blue) and new (Lourantou et al., 2010) (cyan) EDC CO₂ data. Sea level in from corals (green) on Barbados, U-Th dated and uplift-corrected (Peltier and Fairbanks, 2007), and coast line migration (magenta) on the Sunda Shelf (Hanebuth et al., 2000). In (B) sea level is plotted on an individual age scale, but ice core data are plotted on the new synchronised ice core age scale QSR2010 (Lemieux-Dudon et al., 2010). Vertical lines in (B) mark the jump in CO₂ into the B/A as recorded in EDC.

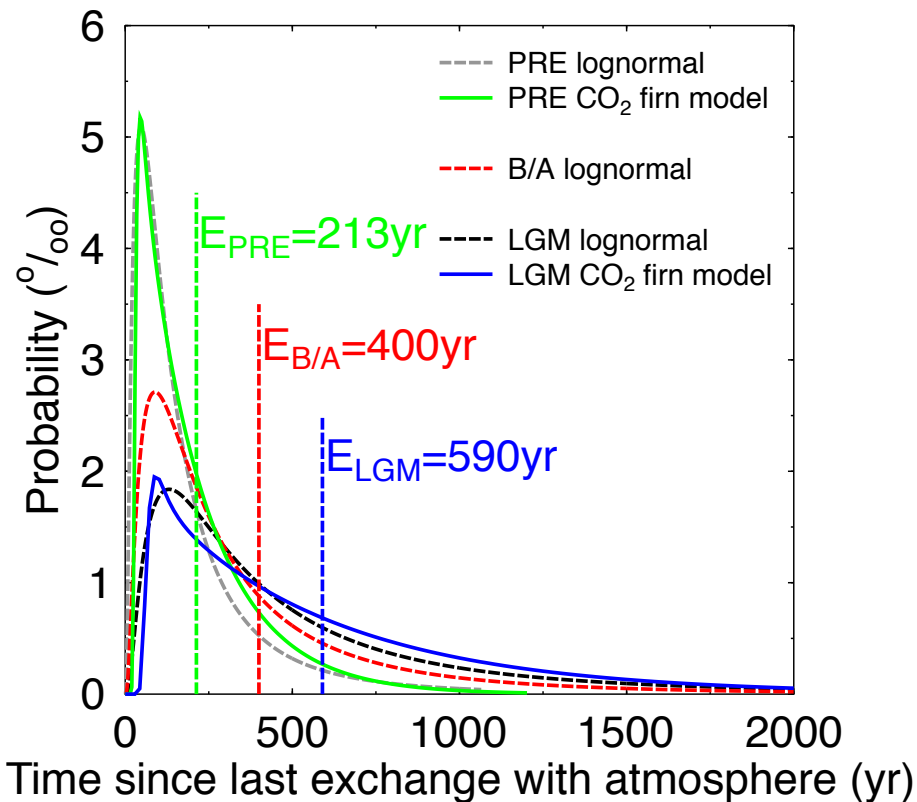


Fig. 2. Age distribution PDF of CO₂ as function of climate state, here pre-industrial (PRE), Bølling/Allerød (B/A) and LGM conditions. Calculation with a firn densification model (Joos and Spahni, 2008) (solid lines, for PRE and LGM) and approximations of all three climate states by a log-normal function (broken lines). For all functions the expected mean values, or width, E are also given.

Rapid rise in CO₂ at the onset of the Bølling/Allerød

P. Köhler et al.

Title Page

Abstract Introduction

Conclusions References

Tables Figures

◀ ▶

◀ ▶

Back Close

Full Screen / Esc

Printer-friendly Version

Interactive Discussion



Rapid rise in CO₂ at the onset of the Bølling/Allerød

P. Köhler et al.

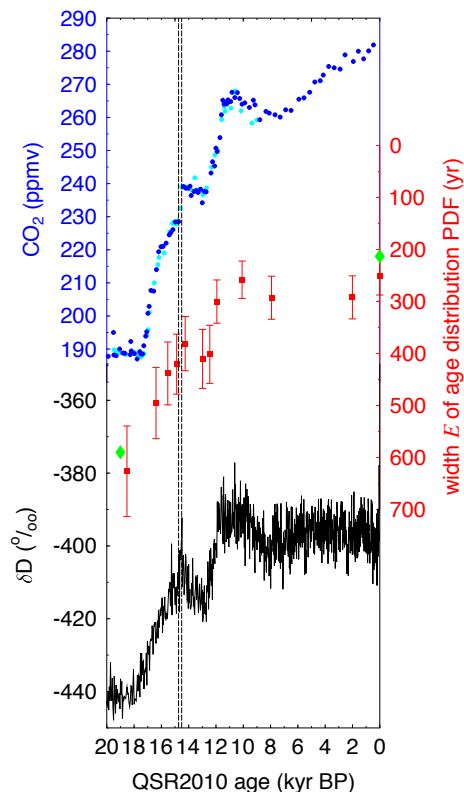


Fig. 3. The evolution of the width E of the age distribution PDF ($\pm 1\sigma$) during the last 20 kyr calculated with a firn densification model including heat diffusion (Goujon et al., 2003). Green diamonds represent the results for the LGM and pre-industrial climate with another firn densification model (Joos and Spahni, 2008). Please note reverse y-axis. Top: EDC CO₂ (Monnin et al., 2001; Lourantou et al., 2010). Bottom: EDC δD data (Stenni et al., 2001). All records on the new age scale QSR2010 (Lemieux-Dudon et al., 2010).

Title Page

Abstract

Introduction

Conclusions

References

Tables

Figures

◀

▶

◀

▶

Back

Close

Full Screen / Esc

Printer-friendly Version

Interactive Discussion



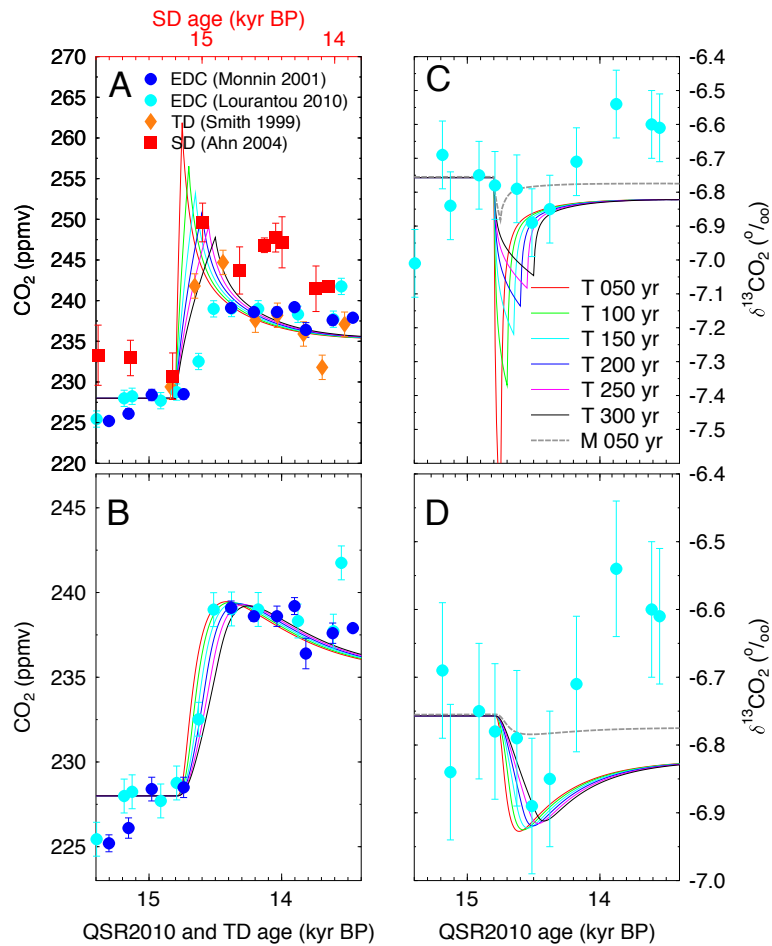


Fig. 4.

Rapid rise in CO₂ at the onset of the Bølling/Allerød

P. Köhler et al.

Title Page

Abstract

Introduction

Conclusions

References

Tables

Figures

◀

▶

◀

▶

Back

Close

Full Screen / Esc

Printer-friendly Version

Interactive Discussion



Rapid rise in CO₂ at the onset of the Bølling/Allerød

P. Köhler et al.

Title Page

Abstract

Introduction

Conclusions

References

Tables

Figures

◀

▶

◀

▶

Back

Close

Full Screen / Esc

Printer-friendly Version

Interactive Discussion



Fig. 4. Simulations with the carbon cycle box model BICYCLE for an injection of 125 PgC into the atmosphere. Injected carbon was either of terrestrial (T: $\delta^{13}\text{C} = -22.5\text{‰}$) or marine (M: $\delta^{13}\text{C} = -8.5\text{‰}$) origin. Release of terrestrial C occurred between 50 and 300 yr. Marine C was released in 50 yr (grey), but is identical to the terrestrial release in A, B. **(A)** Atmospheric CO₂ from simulations and from EDC (Monnin et al., 2001; Lourantou et al., 2010) on the new age scale QSR2010 (Lemieux-Dudon et al., 2010), Siple Dome (Ahn et al., 2004) (SD, own age scale on top x -axis) and Taylor Dome (Smith et al., 1999) (TD, on revised age scale as in Ahn et al., 2004). All CO₂ data synchronised to the CO₂ jump. **(B)** Simulated CO₂ values potentially be recorded in EDC and EDC data. The simulated values are derived by the application of the gas age distribution PDF of the hypothetical atmospheric CO₂ values plotted in (A) followed by a shift in the age scale by the width $E_{B/A} = 400$ yr towards younger ages. **(C, D)** Same simulations for atmospheric $\delta^{13}\text{CO}_2$, cyan dots are new EDC $\delta^{13}\text{CO}_2$ data (Lourantou et al., 2010).

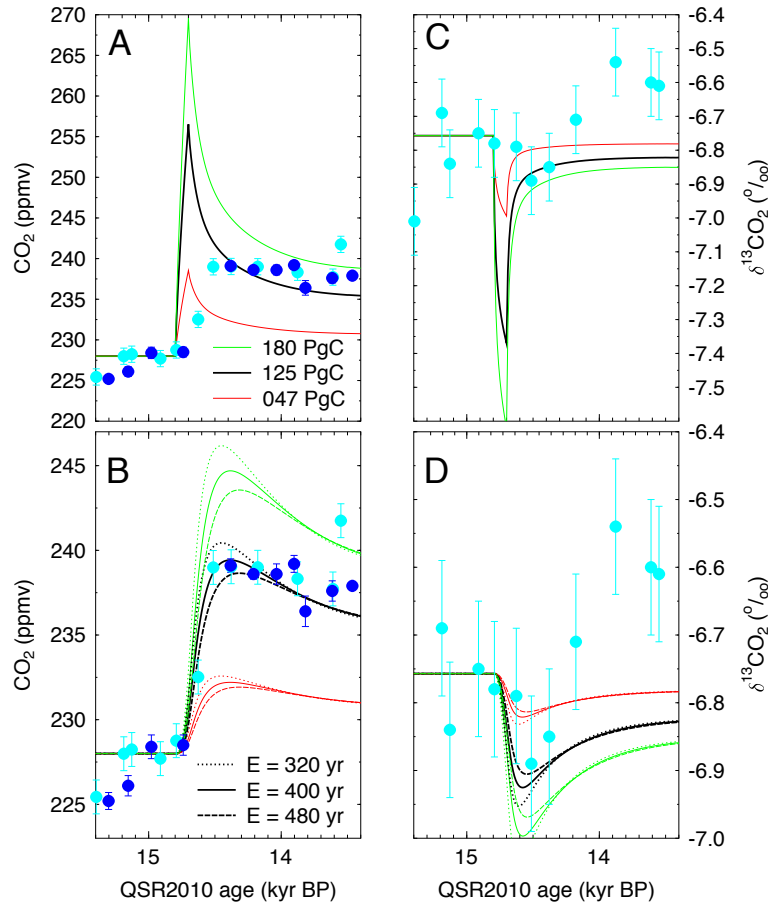


Fig. 5.

Rapid rise in CO₂ at the onset of the Bølling/Allerød

P. Köhler et al.

Title Page

Abstract

Introduction

Conclusions

References

Tables

Figures



Back

Close

Full Screen / Esc

Printer-friendly Version

Interactive Discussion



Fig. 5. Influence of (i) the amount of carbon injected in the atmosphere and of (ii) the details of the gas age distribution on both the atmospheric signal and that potentially recorded in EDC. The amount of carbon injected in the atmosphere (**A, C**) covers the range derived from an airborne fraction f between 12 and 45% from 47 to 180 Pg C with our reference scenario of 125 Pg C in bold. Injections occurred in 100 yr with terrestrial $\delta^{13}\text{C}$ signature. In the filter function of the gas age distribution (**B, D**) the width E varies from 320 yr to 480 yr our best-estimated gas age width E at the onset of the B/A of 400 yr in the solid line, representing the range given by the firn densification model including heat diffusion (Goujon et al., 2003) as plotted in Fig. 3.

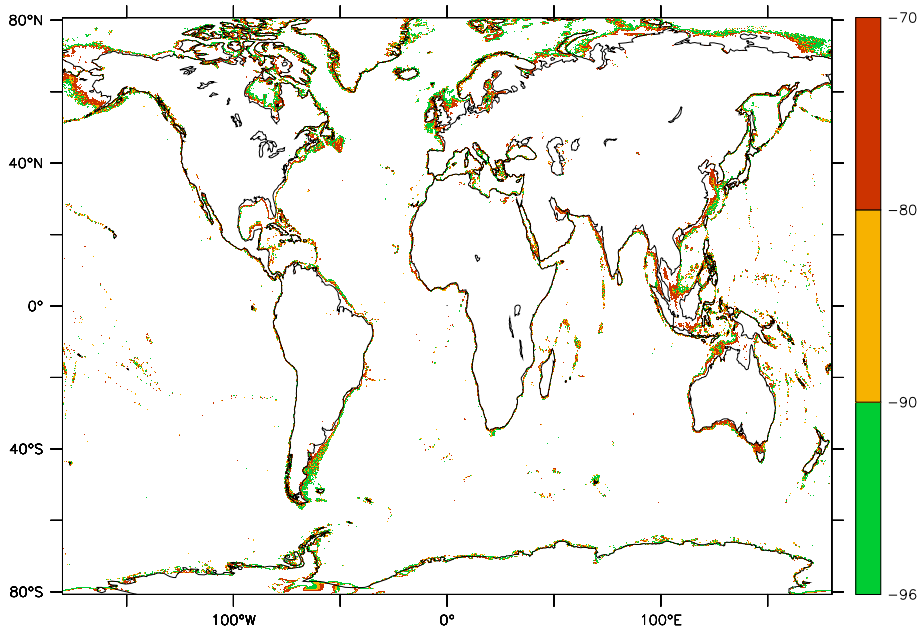


Fig. 6. Areas flooded during MWP-1A. Changes in relative sea level from -96 m to -70 m are plotted from the most recent update (version 12.1) of a global bathymetry (Smith and Sandwell, 1997) with 1 min spatial resolution ranging from 81° S to 81° N.

Rapid rise in CO_2 at the onset of the Bølling/Allerød

P. Köhler et al.

Title Page

Abstract Introduction

Conclusions References

Tables Figures

◀ ▶

◀ ▶

Back Close

Full Screen / Esc

Printer-friendly Version

Interactive Discussion



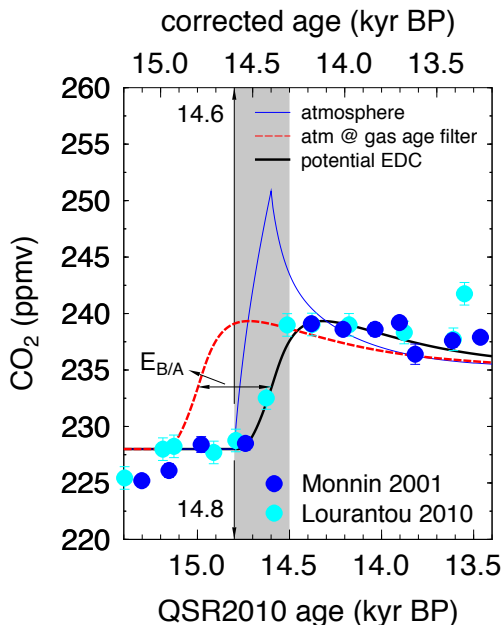


Fig. 7. Influence of the gas age distribution PDF on the CO_2 signal. The original atmospheric signal (blue) leads after filtering with the gas age distribution PDF with the width $E_{B/A}=400$ yr to a time series (red) with similar characteristics (e.g., mean values). To account for the use of the width of the gas age PDF in the gas chronology the resulting curve has to be shifted by $E_{B/A}$ towards younger ages to a time series potentially recorded in EDC (black). This leads to a synchronous start in the CO_2 rise in the atmosphere (blue) and in EDC (black) around 14.8 kyr BP on the ice core age scale QSR2010 (lower x-axis) (Lemieux-Dudon et al., 2010). Due to a similar gas age distribution PDF of CH_4 the synchronisation of ice core data contains a dating artefact which is for EDC at the onset of the B/A around 200 yr (Köhler, 2010). On the age scale corrected for the synchronisation artefact (upper x-axis) the onset in atmospheric CO_2 falls together with the earliest timing of MWP-1A (grey band) (Hanebuth et al., 2000; Kienast et al., 2003).

Rapid rise in CO_2 at the onset of the Bølling/Allerød

P. Köhler et al.

Title Page

Abstract

Introduction

Conclusions

References

Tables

Figures

◀

▶

◀

▶

Back

Close

Full Screen / Esc

Printer-friendly Version

Interactive Discussion

